Saudi Journal of Biological Sciences 26 (2019) 1385–1391

Contents lists available at ScienceDirect

Saudi Journal of Biological Sciences

journal homepage: www.sciencedirect.com

Green synthesis and structural classification of *Acacia nilotica* mediated-silver doped titanium oxide (Ag/TiO_2) spherical nanoparticles: Assessment of its antimicrobial and anticancer activity

Tentu Nageswara Rao [a], Riyazuddin [a], P. Babji [b], Naushad Ahmad [c], Rais Ahmad Khan [c,*], Iftekhar Hassan [d], Syed Ali Shahzad [e], Fohad Mabood Husain [e,*]

[a] Department of School of Material Science and Engineering, Changwon University, South Korea
[b] Department of Physical, Nuclear Chemistry & Chemical Oceanography, Andhra University, India
[c] Department of Chemistry, King Saud University, Riyadh, Saudi Arabia
[d] Department of Zoology, King Saud University, Riyadh, Saudi Arabia
[e] Department of Food Science and Nutrition, King Saud University, Riyadh, Saudi Arabia

ARTICLE INFO

Article history:
Received 9 June 2019
Revised 4 September 2019
Accepted 4 September 2019
Available online 4 September 2019

Keywords:
Green synthesis
Ag/TiO_2
Antimicrobial activity
Anticancer activity
MCF-7
Oxidative stress

ABSTRACT

Current exanimation reports, green fabrication of silver doped TiO_2 nanoparticles (Ag/TiO_2) using aqueous extract of *Acacia nilotica* as bio-reductant and assess its potential as antimicrobial and anticancer agent. The obtained spherical Ag/TiO_2 were characterized by various analytical techniques including FTIR, (XRD), (FE-SEM EDS), and (TEM). Synthesized Ag/TiO_2 demonstrated broad spectrum antibacterial and anticandidal activity. The order of antimicrobial activity was found to be *E. coli* > *C. albicans* > MRSA > *P. aeruginosa*. In addition, cytotoxicity and oxidative stress of Ag/TiO_2 nanoparticles in (MCF-7) cells was also investigated. Outcomes of MTT assay showed concentration dependent reduction in cell viability. Further, synthesized NPs reduced the level of glutathione, induced ROS generation and lipid peroxidation in the treated cells. Therefore, it is envisaged that these spherical nanoparticles may be exploited in drug delivery, pharmaceutical, and food industry.

1. Introduction

Currently, there is a growing interest for the development and use of nanomaterials in various products and technologies. In the last decade, nanoparticles (NPs) have been deployed in the field of biomedical sciences for targeted delivery of drug, imaging, diagnosis and treatment of diseases and development of antimicrobials (Ramar et al., 2015). Metal and metal-oxide nanoparticles demonstrate novel physico-chemical properties that are not associated with individual or bulk molecules (Daniel and Astruc, 2004; Zaman et al., 2016, 2014).

Among NPs, Titanium oxide (TiO_2) NPs (titanium dioxide nanoparticles) demonstrate unique surface chemistry, morphologies and have been used mainly in textile, paper, cosmetics and food industries (Julkapli et al., 2014). Most of the TiO_2 NPs are synthesized using physico-chemical methods that necessitate high temperature with pressure and toxic chemicals which make them unsuitable for use as medicine and other biomedical application (Abbasi et al., 2018). Hence the focus has shifted to the use of eco-friendly and cost-effective approaches to synthesize nano sized TiO_2 particles. One such method of synthesis employs plant extracts as reducing agent and a single reducing agent can be used to produce various NPs. Moreover, this green synthesis approach yields NPs with better morphology and stability (Bhainsa and D'Souza, 2006). Recently, TiO_2-NPs have been synthesized from a range of plants including *Nyctanthes arbortristis* extraction of leaf (Sundrarajan and Gowri, 2011), aqueous extract of *Catharanthus roseus* (leaf) (Bagavan et al., 2011), *Eclipta prostrata* aqueous leaf extract (Rajakumar et al., 2012), *Azadirchta indica* (Sankar et al., 2015) for various applications. Further, the novel metal doping of TiO_2 improves the efficiency of NPs by manipulating the band gap energy. Amongst NPs, silver doped titanium oxide NPs

* Corresponding authors.
E-mail addresses: krais@ksu.edu.sa (R.A. Khan), fhusain@ksu.edu.sa (F.M. Husain).
Peer review under responsibility of King Saud University.

Production and hosting by Elsevier

https://doi.org/10.1016/j.sjbs.2019.09.005
1319-562X/

(Ag/TiO_2 NPs) has gained special attention due to its non-toxic nature, low cost of synthesis and high availability (Zhang et al., 2008). Ag/TiO_2 NPs have been previously synthesized using the extracts of *Citrus limon* and *Nephelium lappaceum* and reported for improved photocatalytic activity (Kumar et al., 2016; Liang et al., 2012). Nevertheless, limited reports have emerged regarding green synthesis of Ag/TiO_2-NPs using plant extracts as biological reductants. Owing to the limited information on the usage of plant extracts for synthesizing in Ag/TiO_2-NPs, doped NPs were synthesized using extract of *Acacia nilotica* using a cost effective and eco-friendly approach. Further, these NPs were characterized employing XRD, FE-EDS, TEM and FTIR spectroscopic techniques. Further, since most of studies related to Ag/TiO_2 NPs have been centered around photo catalysis, we have explored the bactericidal and fungicidal potential as well as its role as anti-cancer chemotherapeutic using breast cancer cell line (MCF-7).

2. Materials and methods

Aerial parts of *Acacia nilotica* were collected from the campus of Andhra University, Visakhapatnam, India. Tetrabutyl orthotitanate ($C_{16}H_{36}O_4Ti$, 99.9%), silver nitrate ($AgNO_3$, 99.5%) were obtained from Merck Ltd, India. Lyophilized culture of microorganisms was acquired from Microbiology Department of Andhra University.

2.1. Preparation of extract Acacia nilotica

The aerial parts of *Acacia nilotica* were cleaned with water for 3 times and followed by deionized water to clean the dust; plant leaves were sheltered, dried totally for 7 days to drain out moisture and then ground to powder. The 10 g of powdered sample was added to 50 ml of double distilled water (DDW) and left for incubation and intermittent stirring was done. Sample was boiled for one hour, cooled to room temperature and filtered using Whatman filter paper, and filtrate used for the synthesis of silver doped TiO_2-NPs.

2.2. Green synthesis of silver doped TiO_2 spherical nanoparticles (Ag/TiO_2)

Ag/TiO_2 NPs were synthesized using silver nitrate, Tetrabutyl orthotitanate and extract of *Acacia nilotica*. In short, 20 mM tetrabutyl orthotitanate was added dropwise into 50 ml absolute ethanol, stirred vigorously for 20 min at room temperature and after that few drops of 65% HNO_3 was added. *Acacia nilotica* extract (1 mM) and 1 mM of Silver nitrate ($AgNO_3$) were added to the previously prepared mixture and stirred for 1 h. Subsequently, deionized water was added to the mixture and the consequent solution was shaken for couple of hours at room temperature (RT) for the gel formation, this gel was kept for 1 day at RT. After drying at 80 °C for 1 day, the as-prepared *Acacia* extract and Ag/TiO_2 samples were obtained and then annealed at 400 °C for 3 h to give a greyish material.

2.3. Characterization of spherical Ag/TiO_2 NPs

Documentation of crystal phases and determination of average crystalline size was performed using powder XRD (X-ray diffraction). Diffractions dimensions were achieved through PANalytical PW 3040/60 X'Pert PRO instrument using Ni-filtered Cu-Kα radiation (1.54 Å) curve fitting and integration was used for X'Pert high score plus software. The FESEM (Filed Emission Scanning Electron Microscopy) was done to study the morphology and elements identification were done by EDS (Energy Dispersion Spectroscopy) on JEOL JEM-2300, of the NPs. TEM (Transmission Electron Microscopy) gave the size and SAED (selective area electron diffraction) pattern at a voltage of 200 kV on JEOL JEM-1200EX (Japan). FT-IR analysis was carried out on a Perkin Elmer FTIR spectrophotometer spectrum two (Perkin Elmer Life and Analytical Sciences, CT, USA).

2.4. Antimicrobial studies

Synthesized Ag/TiO_2 NPs were assessed for their bactericidal and fungicidal potential using agar well diffusion assay in contradiction of human pathogens namely MRSA, Gram positive, *E. coli* ATCC 25922, *P. aeruginosa* ATCC 27853 (Gram negative) and *C. albicans* ATCC 10231 (fungi). Each strain was wiped on to Mueller Hinton agar and wells of 10 mm were punched. Synthesized NPs (100 μl) were loaded in wells and at 37 °C, plates were incubated for 1 day. Halo zone surrounding the well was measured to determine the antimicrobial activity.

Minimum inhibitory concentration of synthesized NPs was determined against test microbial strains using standard method described previously (Al-Shabib et al., 2019).

2.5. In vitro anti-proliferative/anticancer studies

Cells (MCF-7) were grown and maintained in DMEM under anaeribic conditions at 37 °C and cell-viability was evaluated using dye Trypan blue (Siddiqui et al., 2008).

2.6. Cytotoxicity by MTT assay

Cytotoxicity of the synthesized NPs was determined using MTT-assay (Siddiqui et al., 2008). Briefly, 1×10^3 cells were plated and allowed to adhere in 96-well plate under anaerobic conditions as described previously. Post incubation, 10-μL of MTT solution was added in each well to make incubation for 4-hours in a CO_2 incubator. Subsequently, 200-μL of DMSO was added to each well after discarding supernatant. The development of the color was read at 550 nm.

2.7. Miscroscopic analysis of cell morphology

Changes in morphology of under study cells brought about by the treatment with varying concentrations of Ag/TiO_2 NPs was observed using phase contrast inverted microscope.

2.8. GSH levels

Cells treated with Ag/TiO_2 NPs were centrifuged and cellular protein was precipitated. Subsequently, 0.4 M, (pH-8.9) Tris buffer and DTNB were added to the supernatant sequentially and left for incubation on shaking for 10 min at 37 °C. Color development was measured at 412 nm (Chandra et al., 2002).

2.9. Lipid peroxidation

Lipid peroxidation (LPO) was determined with TBARS assay. Ag/TiO_2 exposed cells were centrifuged, sonicated and again centrifuged. Thiobarbituric acid (TBA) (2 ml) was added to the resulting supernatant (1 ml) and heated at 100 °C for 15 mins. Samples were then cooled and centrifuged and absorbance of the resulting supernatant was read at 550 nm (Grossberg, 1981).

3. Results and discussion

3.1. Powder XRD of Ag/TiO2 NPs

Fig. 1a and 1b presents the XRD pattern of pure TiO_2 and synthesized Ag/TiO_2. Well defined diffraction peaks with 2θ are at about 25.35°, 38.08°, 48.08°, 54.19°, 54.95°, 62.63°, 68.21°,

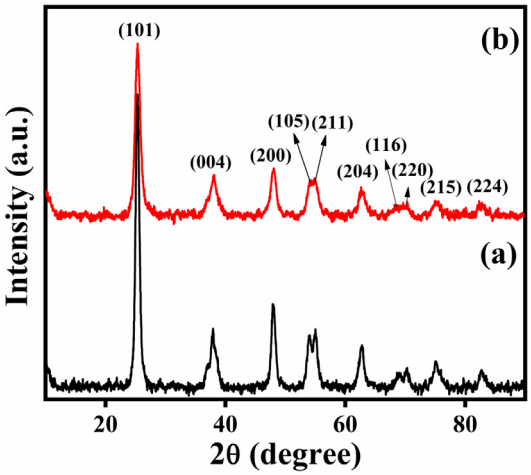

Fig. 1. XRD-pattern for (a) Pure TiO_2; (b) Ag/TiO_2 NPs.

70.39°, 74.94° & 82.73° are allocated for (1 0 1), (0 0 4), (2 0 0), (1 0 5), (2 1 1), (2 0 4), (1 1 6), (2 2 0), (2 1 5) & (2 2 4) crystal planes, respectively. The pattern of XRD is in agreement with the tetragonal structure of anatase TiO_2 (JCPDS# 21-1272). No peak for silver was observed, which indicates that it is well dispersed in TiO_2 matrix in the form of minor cluster. The average size of crystallite NPs samples were measured from reflection plane (1 0 1) using Debye-Scherrer equation (Dhage et al., 2004). It was found to be around 9 nm and 17 nm of pure Titanium oxide and doped Ag/TiO_2, respectively. The details of lattice parameters are presented in Table 1. The tetragonal structure for TiO_2 has unit cell edge '*a*' = '*b*' is 3.785 Å and '*c*' is 9.514 Å and this value is calculated theoretically using formula:

$$1/d_{hkl} = (h^2 + k^2)/a^2 + l^2/c^2$$

The experimental lattice constants '*a*', '*b*' and 'c' is calculated from the XRD peak (1 0 1), (0 0 4) and (2 0 0) of the XRD pattern '*a*' = '*b*' is 3.780 Å, '*c*' is 9.444 Å, and unit cell volume is V = 134.94 Å. Both theoretical and experimental lattice constants are in well agreements.

3.2. FE-SEM

Surface morphology was determined with FESEM. The synthesized Ag/TiO_2 were distributed irregularly having rough surface (Fig. 2a). Synthesized NPs were circular in shape with an average size of 11.25 nm. However, larger particles of Ag/TiO_2 were also noticed possibly due to the aggregation of NPs during the preparation of samples. Chemical composition of synthesized NPs was determined with EDS (Fig. 2b). EDS spectrum shows presence of Ag & Ti peaks around 3 eV and 4.5 eV, respectively. EDS spectrum analysis also revealed that silver is in metallic form and free from impurities.

3.3. Transmission electron microscopy

TEM pictures demonstrated the presence of polycrystalline Ag/TiO_2 NPs (Fig. 3a). The biosynthesized nanoparticles were predominately spherical in shape with an average size of 20–40 nm (Fig. 3c) and some were agglomerated revealing a strong interaction with the molecules of *Acacia* extract.

SAED pattern exhibits discrete circular diffraction rings corresponding to anatase phase (Fig. 3b). Obtained polycrystalline diffraction rings of fabricated spherical NPs were in agreement with the earlier study.

3.4. FTIR

Fig. 4 demonstrates FTIR spectra of pure TiO_2 & Ag doped TiO_2-NPs. The absorbance bands appear in spectrum of un-doped TiO_2 at 3387, 2925, 2853, 1627, 1383, 662, 626, 584, and 552 cm^{-1}. The wide bands observed at 3387, 2925 and 2853 cm s^{-1} could be assigned to vibration bands of O-H groups in un-doped TiO_2. Groups at 2853 cm s^{-1} resemble to lopsided extending, distorting, and shaking methylene vibrations gatherings, separately. Peaks at 1068 and 1028 cm^{-1} are due to the C—O stretching vibration of ether and alcoholic gatherings, individually (Prasad et al., 2007) and 500–900 cm^{-1} Ti—O—Ti (Ding et al., 2000; Liu et al., 2007). While, Ag/TiO_2 nanoparticles indicated characteristic signals at 3416, 2920, 2852, 2326, 2111, 1635, 1462, 1384, 1097, 1018, 663, 606 cm^{-1}. IR range of nanoparticles, a shift in the

Table1
Lattice parameters for pure TiO_2 and doped Ag/TiO_2.

	2θ	D	FWHM of intense peak β (radians)	Size of the crystallite (D) nm	Lattice Parameters Å	hkl
Pure TiO_2	25.28	3.520	0.0083	17	$a = b = 3.7852$ $c = 9.5139$	101
Ag/TiO_2	25.35	3.511	0.0166	9	$a = b = 3.780$ $c = 9.444$	101

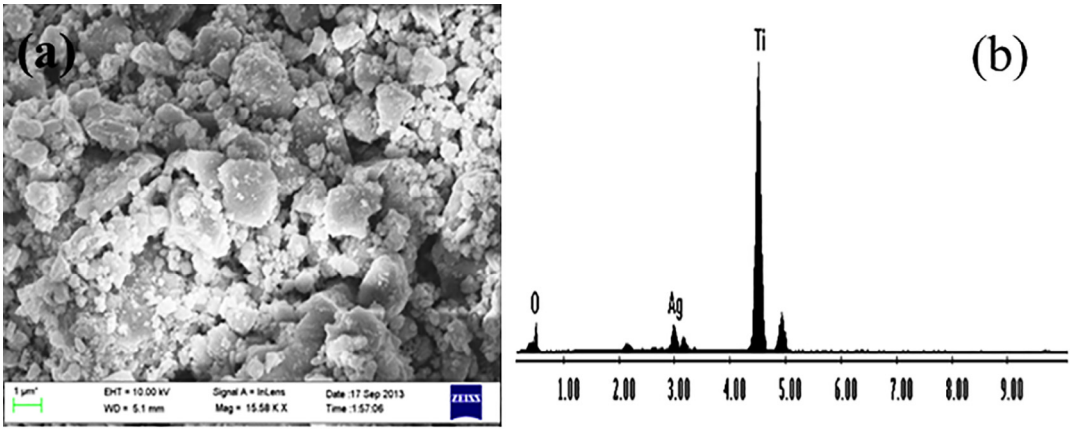

Fig. 2. (a) FE-SEM micrograph-Ag/TiO_2-NPs and (b) EDS synthesized Ag/TiO_2-NPs.

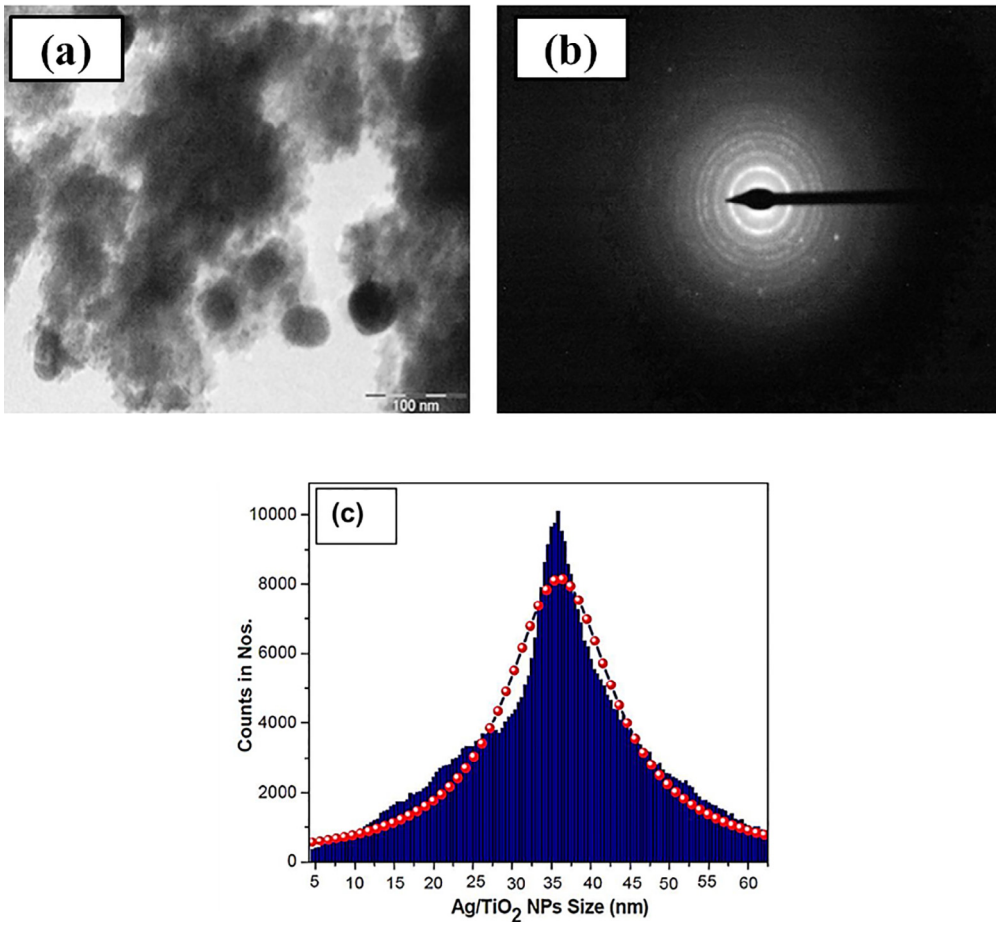

Fig. 3. (a) TEM micrograph of Ag/TiO_2, (b) SAED pattern of Ag/TiO_2-NPs and (c) Size distribution curve.

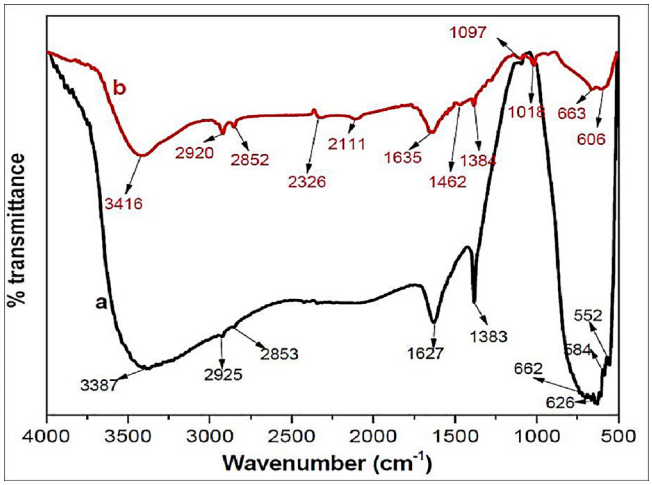

Fig. 4. (a) FTIR spectra of pure TiO_2 and (b) FTIR spectra of synthesized Ag/TiO_2 nanoparticles.

absorbance tops was watched a solid expansive band at 3416 cm^{-1} could be credited to the extending vibration of the hydroxyl gathering and the interlayer water molecules (Li et al., 2008). This marvel was essentially brought about through Ti—O—H extending vibration. Close band 1635 cm s^{-1} for example could be appointed for twisting the vibration of H—O—H bond on TiO_2 catalyst (Jensen and Fuierer, 2006) and at 1384 cm^{-1} proposing the official of Ag—O—Ti individually. The solid groups at 2920, 2852 cm^{-1} relate to nearness of C—H extended vibration for CH_3, CH_2 and C—H extending vibrations of alkane and aldehydes and 1635 cm^{-1} is doled out to the twisting recurrence of O—H bond in H_2O; while the situated band near 1384 cm s^{-1} compared with a vibration for Ti-ligand bond. Further, the event of the crest at 2326 cm^{-1} and 2111 cm^{-1} is nearness of transitional metal carbonyls affirm the decrease of silver particles, coupled for oxidation of hydroxyl and carboxyl gatherings, demonstrative for all broadly oxidized nature of acacia separate. Bands at 1462 cm^{-1} relates to asymmetric and at 663 cm^{-1} compares to anatase pinnacle of TiO_2 (Jensen and Fuierer, 2006).

3.5. Antimicrobial studies

Antibacterial activity of synthesized Ag/TiO_2-NP_S were studied amongst both (Gram positive and Gram negative) pathogenic bacteria. Further, opportunistic pathogenic yeast *C. albicans* was also used to investigate antifungal potential. Ag/TiO_2 NPs showed maximum zone of inhibition against *E. coli* (24 mm) followed by *C. albicans* (22 mm), methicillin resistant *S. aureus* (20 mm) and least was observed against *P. aeruginosa* (15 mm) at 500 μg/ml concentration (Fig. 5). Antibiotics were used as positive control (data not shown). Results of the antimicrobial activity are in agreement with the report on antibacterial activity of TiO_2 NPs against drug resistant bacteria (Jesline et al., 2015; Murugan et al., 2016). Minimum inhibitory concentration of Ag/TiO_2 NPs was also determined against all test pathogens. MIC was found to be 64 μg/ml against *E. coli*, *S. aureus* and *C. albicans* while 128 μg/ml against *P. aeruginosa*. The Antimicrobial activity of Ag/TiO_2-NPs are generally credited

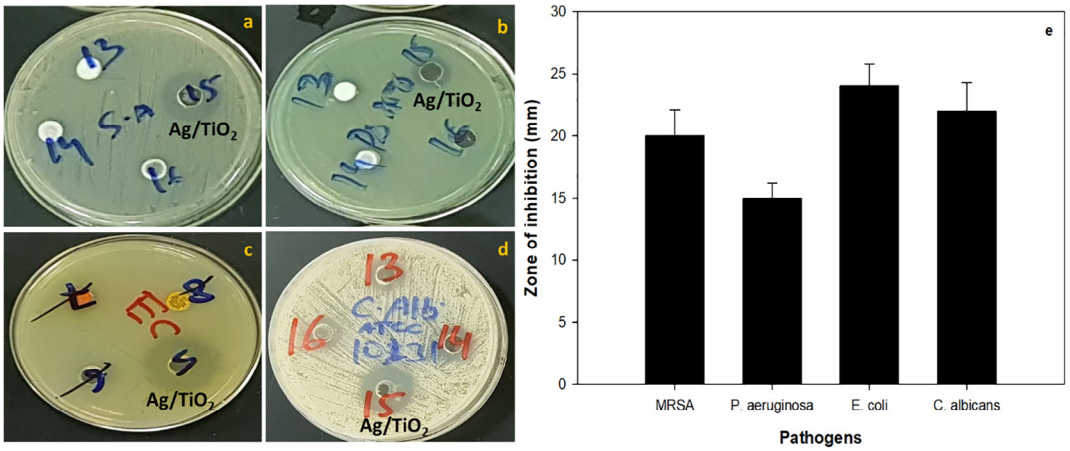

Fig. 5. Antimicrobial activity for Ag/TiO_2 NPs using agar well-diffusion method against (a) MRSA, (b) *P. aeruginosa*, (c) *E. coli*, (d) *C. albicans*, and (e) bar diagram depicting the zone of inhibition (mm) of Ag/TiO_2 NPs against various pathogens.

to disrupting membrane integrity by reactive oxygen species (ROS) leading for phospholipid peroxidation and ultimately leads to cell-death (Jacob Inbaneson et al., 2011).

3.6. In vitro Anti-proliferative/anticancer activity

3.6.1. MTT assay for cytotoxicity

The cytotoxicity of Ag/TiO_2 NPs was verified amongst MCF-7 cell-lines by exposing 10–100 μM concentrations of NPs for 1 day using the MTT-assay. Concentration dependent cytotoxicity was recorded after exposing the cell lines to 10, 25, 50 and 100 μM concentrations of synthesized NPs (Fig. 6).

Histogram (Fig. 6a) very clearly demonstrates that with the increase in concentration of Ag/TiO_2-NPs, there is progressive decrease in percentage cell viability. Upon increasing the concentration the adsorption of NPs on cell membranes increases, leading to enhanced penetration, facilitating binding to the bases of DNA and causing cell death. Ag/TiO_2 NPs demonstrated

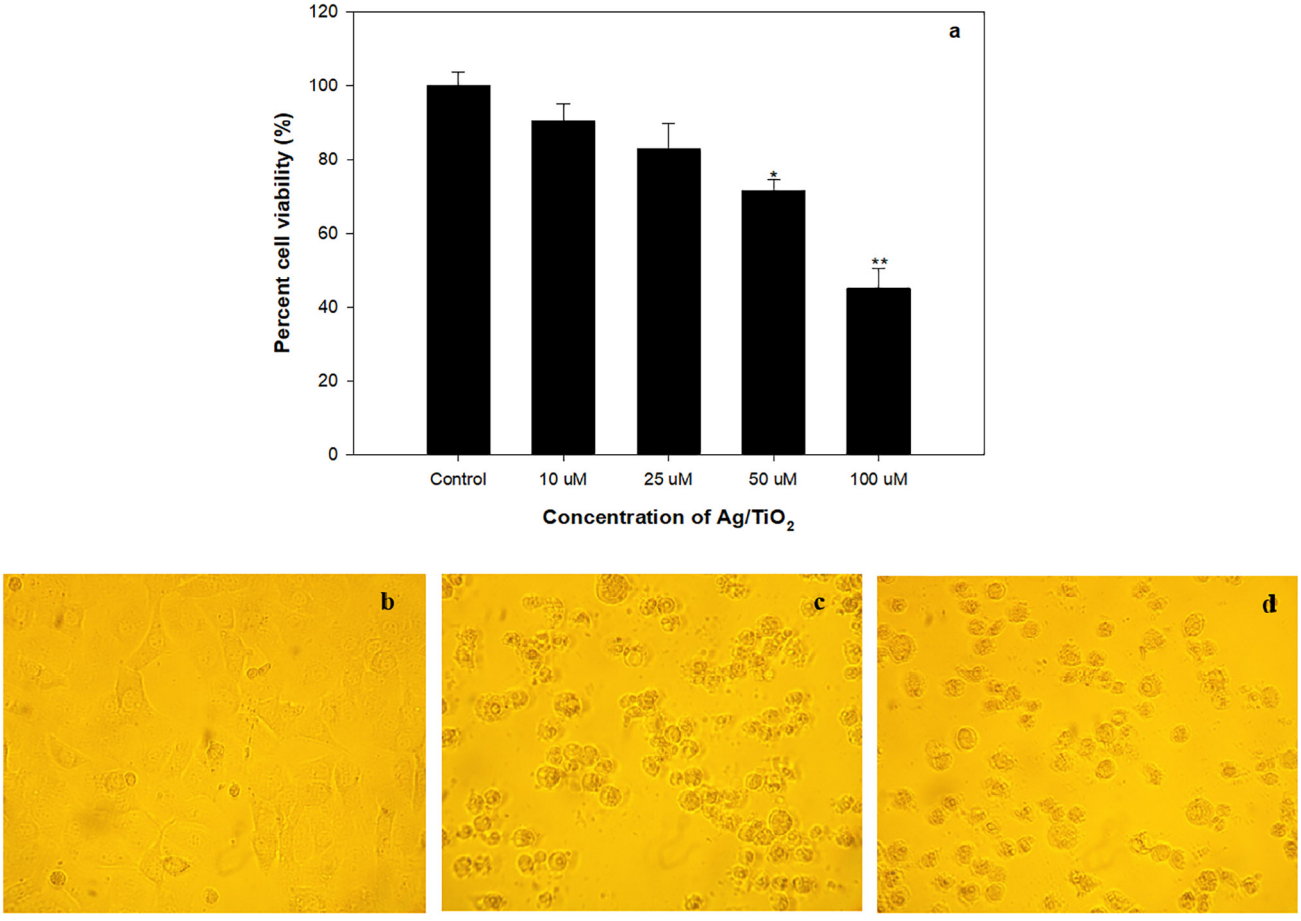

Fig. 6. Cytotoxicity assessment using MTT assay. (a) MCF7 cells exposed to varying concentrations of synthesized Ag/TiO_2 for 24 h. *$p < 0.01$, **$p < 0.005$. The morphological analysis using phase contrast microscopy (b) untreated control, (c) Ag/TiO_2 50 μM and (d) Ag/TiO_2 100 μM.

concentration-dependent cytotoxic profile in MCF-7 cell lines. The microscopic analysis to observe morphological changes showed that the cell proliferation was significantly reduced. Cell shrinkage and cell detachment was also observed, as depicted in Fig. 6b–d. Similar concentration dependent cytotoxicity against MCF-7 cells was demonstrated by hydrothermally synthesized TiO_2 NPs (Murugan et al., 2016)

3.6.2. Intracellular Glutathione (GSH) depletion

Almost all mammalian cell types possess GSH as an important oxidant scavenger. GSH redox is a key player in many biological processes such as activation of genes at transcription level, regulation of signal transduction pathways that are redox-related, control of cell-proliferation and apoptosis. GSH/GSSG ration in the cancer cells were well-known for regulating cell cycle, mutagenisis, synthesis of DNA, growth, resistance to drugs and radiation. Tumor tissues have elevated GSH levels than their normal counterparts (Dharmaraja, 2017; Kawahara et al., 2017; Usman et al., 2017). Recently, the impact of intracellular GSH in the anticancer therapy has been highlighted as cytotoxicity of most anti-proliferative drugs depends on levels of intracellular GSH. It is envisaged that reduced GSH levels in cells treated with Ag/TiO_2 is indicative of the effective anticancer therapy, if the cytotoxicity is induced by oxidative stress. Therefore, cells in GSH levels were exposed to Ag/TiO_2-NP_s was determined. Results of glutathione depletion in cultured MCF-7 cells were exposed to Ag/TiO_2-NP_s are depicted in Fig. 7. Statistically significant reduction (67%) in GSH level was recorded at 100 μM while 35% decrease was observed at 50 μM. In another study, reduced GSH levels in MCF-7 cells treated with silver doped TiO_2 NPs has been reported previously (Ahamed et al., 2017). Our results corroborate well with the findings of Ahamed et al. (2017).

3.7. Lipid Peroxidation

Lipid Peroxidation (LPO), occurs due to the generation of ROS in the structure and function of cell-membrane. A well documented fact is that ROS, lipid hydroperoxides and oxygenated product of lipid degradation can contribute in signal transduction cascade, cell-proliferation, differentiation, maturation and apoptosis (Barrera et al., 2004; Cejas et al., 2004; Gago-Dominguez et al., 2007). Therefore, influence of Ag/TiO_2 NPs on LPO in MCF-7 cells was assessed, Lipid peroxidation increased substantially with increase in concentration of Ag/TiO_2 NPs (50 and 100 μM) as summarized in Fig. 8. Increase in lipid peroxidation in MCF-7 cells after treatment with $AgTiO_2$ NPs could be attributed to ROS generation.

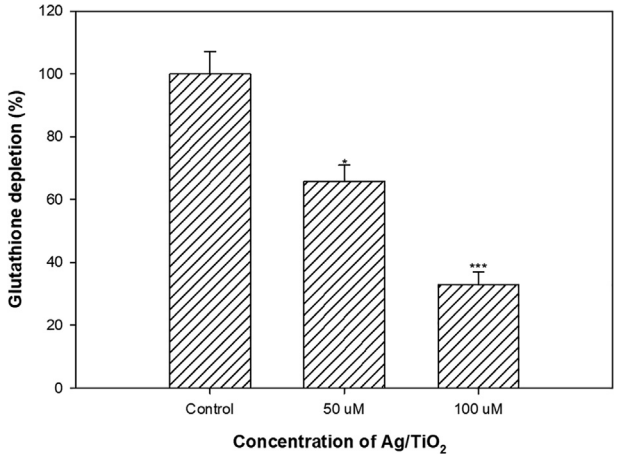

Fig. 7. Percent change in the levels of glutathione in MCF-7 cells treated with different concentrations of Ag/TiO_2 NPs. *p < 0.01, ***p < 0.001.

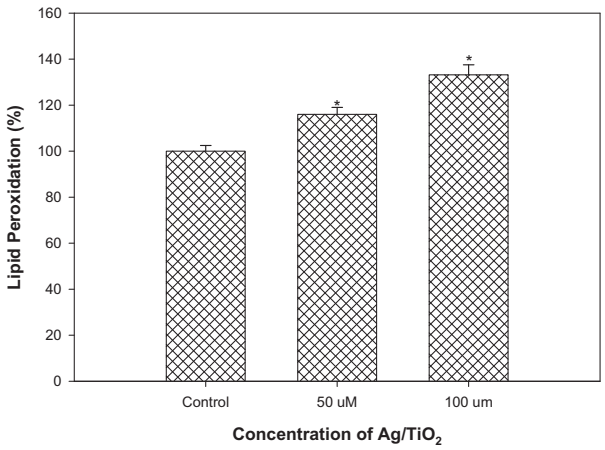

Fig. 8. Percentage change in lipid-peroxidation in MCF-7 cells exposed to Ag/TiO_2 NPs. *p < 0.01.

4. Conclusion

In the present investigation, we report a simple, safe, environment friendly and economical biological technique for synthesizing Ag-doped TiO_2-NPs with *Acacia nilotica* extraction. Synthesized material were well-characterized using enormous spectroscopic and microscopic methods viz. FTIR, XRD, FESEM, EDS and TEM. $AgTiO_2$ NPs were assessed for their antimicrobial action and the NPs demonstrated significant antibacterial as well as antifungal activity against pathogenic microorganisms. Further, our findings on anticancer/anti-proliferative activity demonstrated that $AgTiO_2$ NPs induce cytotoxicity in MCF-7 (human breast adenocarcinoma) cell lines, which is mediated by generation of ROS and oxidative stress. Therefore, it is envisaged that these Ag-doped TiO_2 nanoparticles may be exploited in drug delivery, pharmaceutical and food industry.

Declaration of Competing Interest

The authors declared that there is no conflict of interest.

Acknowledgement

Authors extend their appreciation to the Deanship of Scientific Research at King Saud University for funding the work through the research group Project No. RG-1440-059.

References

Abbasi, B.H., Hashmi, S.S., Zahir, A., Hano, C., Ahmad, W., Nadeem, M., Tungmunnithum, D., 2018. The current trends in the green syntheses of titanium oxide nanoparticles and their applications. Green Chem. Lett. Rev. 11, 492–502. https://doi.org/10.1080/17518253.2018.1538430.

Ahamed, M., Khan, M.A.M., Akhtar, M.J., Alhadlaq, H.A., Alshamsan, A., 2017. Ag-doping regulates the cytotoxicity of TiO_2 nanoparticles via oxidative stress in human cancer cells. Sci. Rep. 7, 1–14. https://doi.org/10.1038/s41598-017-17559-9.

Al-Shabib, N.A., Husain, F.M., Khan, R.A., Khan, M.S., Alam, M.Z., Ansari, F.A., Laeeq, S., Zubair, M., Shahzad, S.A., Khan, J.M., Alsalme, A., Ahmad, I., 2019. Interference of phosphane copper (I) complexes of β-carboline with quorum sensing regulated virulence functions and biofilm in foodborne pathogenic bacteria: a first report. Saudi J. Biol. Sci. 26, 308–316. https://doi.org/10.1016/j.sjbs.2018.04.013.

Bagavan, A., Kirthi, A.V., Velayutham, K., Rahuman, A.A., Zahir, A.A., Marimuthu, S., Jayaseelan, C., Rajakumar, G., Elango, G., Santhoshkumar, T., Kamaraj, C., 2011. Evaluation of Catharanthus roseus leaf extract-mediated biosynthesis of

titanium dioxide nanoparticles against Hippobosca maculata and Bovicola ovis. Parasitol. Res. 111, 2329–2337. https://doi.org/10.1007/s00436-011-2676-x.
Barrera, G., Pizzimenti, S., Dianzani, M.U., 2004. 4-Hydroxynonenal and regulation of cell cycle: effects on the pRb/E2F pathway. Free Radic. Biol. Med. 37, 597–606. https://doi.org/10.1016/j.freeradbiomed.2004.05.023.
Bhainsa, K.C., D'Souza, S.F., 2006. Extracellular biosynthesis of silver nanoparticles using the fungus Aspergillus fumigatus. Colloids Surf. B Biointerfaces 47, 160–164. https://doi.org/10.1016/j.colsurfb.2005.11.026.
Cejas, P., Casado, E., Belda-Iniesta, C., Castro, J. De, Espinosa, E., Redondo, A., Sereno, M., García-Cabezas, M.Á., Vara, J.A.F., Domínguez-Cáceres, A., Perona, R., González-Barón, M., 2004. Implications of oxidative stress and cell membrane lipid peroxidation in human cancer (Spain). Cancer Causes Control 15, 707–719. https://doi.org/10.1023/B:CACO.0000036189.61607.52.
Chandra, D., Ramana, K.V., Wang, L., Christensen, B.N., Bhatnagar, A., Srivastava, S.K., 2002. Inhibition of fiber cell globulization and hyperglycemia-induced lens opacification by aminopeptidase inhibitor bestatin. Investig. Ophthalmol. Vis. Sci. 43, 2285–2292.
Daniel, M.-C., Astruc, D., 2004. Gold nanoparticles: assembly, supramolecular chemistry, quantum-size-related properties, and applications toward biology, catalysis, and nanotechnology. Chem. Rev. 104, 293–346. https://doi.org/10.1021/cr030698+.
Dhage, S.R., Gaikwad, S.P., Ravi, V., 2004. Synthesis of nanocrystalline TiO_2 by tartarate gel method. Bull. Mater. Sci. 27, 487–489. https://doi.org/10.1007/BF02707273.
Dharmaraja, A.T., 2017. Role of reactive oxygen species (ROS) in therapeutics and drug resistance in cancer and bacteria. J. Med. Chem. 60, 3221–3240. https://doi.org/10.1021/acs.jmedchem.6b01243.
Ding, Z., Lu, G.Q., Greenfield, P.F., 2000. <Jp993819B.Pdf> 4815–4820.
Gago-Dominguez, M., Jiang, X., Castelao, J.E., 2007. Lipid peroxidation, oxidative stress genes and dietary factors in breast cancer protection: a hypothesis. Breast Cancer Res. 9, 201. https://doi.org/10.1186/bcr1628.
Grossberg, S.E., 1981. Thiobarbituric acid assay. Methods 78, 369–373.
Jacob Inbaneson, S., Ravikumar, S., Manikandan, N., 2011. Antibacterial potential of silver nanoparticles against isolated urinary tract infectious bacterial pathogens. Appl. Nanosci. 1, 231–236. https://doi.org/10.1007/s13204-011-0031-2.
Jensen, M.J., Fuierer, P.A., 2006. Low-temperature preparation of nanocrystalline anatase films through a sol-gel route. J. Sol.–Gel. Sci. Technol. 39, 229–233. https://doi.org/10.1007/s10971-006-7837-5.
Jesline, A., John, N.P., Narayanan, P.M., Vani, C., Murugan, S., 2015. Antimicrobial activity of zinc and titanium dioxide nanoparticles against biofilm-producing methicillin-resistant Staphylococcus aureus. Appl. Nanosci. 5, 157–162. https://doi.org/10.1007/s13204-014-0301-x.
Julkapli, N.M., Bagheri, S., Bee, S., Hamid, A., 2014. Recent advances in heterogeneous photocatalytic decolorization of synthetic dyes. Sci. World J. https://doi.org/10.1155/2014/692307.
Kawahara, B., Moller, T., Hu-Moore, K., Carrington, S., Faull, K.F., Sen, S., Mascharak, P.K., 2017. Attenuation of antioxidant capacity in human breast cancer cells by carbon monoxide through inhibition of cystathionine β-synthase activity: implications in chemotherapeutic drug sensitivity. J. Med. Chem. 60, 8000–8010. https://doi.org/10.1021/acs.jmedchem.7b00476.
Kumar, B., Smita, K., Angulo, Y., Cumbal, L., 2016. Valorization of rambutan peel for the synthesis of silver-doped titanium dioxide (Ag/TiO_2) nanoparticles. Green Process. Synth. 5, 371–377. https://doi.org/10.1515/gps-2016-0003.
Li, Y., Ma, G., Peng, S., Lu, G., Li, S., 2008. Boron and nitrogen co-doped titania with enhanced visible-light photocatalytic activity for hydrogen evolution. Appl. Surf. Sci. 254, 6831–6836. https://doi.org/10.1016/j.apsusc.2008.04.075.
Liang, W., Church, T.L., Harris, A.T., 2012. Biogenic synthesis of photocatalytically active Ag/TiO_2 and Au/TiO_2 composites. Green Chem. 14, 968–975. https://doi.org/10.1039/c2gc16082j.
Liu, J., Li, X., Zuo, S., Yu, Y., 2007. Preparation and photocatalytic activity of silver and TiO_2 nanoparticles/montmorillonite composites. Appl. Clay Sci. 37, 275–280. https://doi.org/10.1016/j.clay.2007.01.008.
Murugan, K., Dinesh, D., Kavithaa, K., Paulpandi, M., Ponraj, T., Alsalhi, M.S., Devanesan, S., Subramaniam, J., Rajaganesh, R., Wei, H., Kumar, S., Nicoletti, M., Benelli, G., 2016. Hydrothermal synthesis of titanium dioxide nanoparticles: mosquitocidal potential and anticancer activity on human breast cancer cells (MCF-7). Parasitol. Res. 115, 1085–1096. https://doi.org/10.1007/s00436-015-4838-8.
Prasad, K., Jha, A.K., Kulkarni, A.R., 2007. Lactobacillus assisted synthesis of titanium nanoparticles. Nanoscale Res. Lett. 2, 248–250. https://doi.org/10.1007/s11671-007-9060-x.
Rajakumar, G., Rahuman, A.A., Priyamvada, B., Khanna, V.G., Kumar, D.K., Sujin, P.J., 2012. Eclipta prostrata leaf aqueous extract mediated synthesis of titanium dioxide nanoparticles. Mater. Lett. 68, 115–117. https://doi.org/10.1016/j.matlet.2011.10.038.
Ramar, M., Manikandan, B., Marimuthu, P.N., Raman, T., Mahalingam, A., Subramanian, P., Karthick, S., Munusamy, A., 2015. Synthesis of silver nanoparticles using Solanum trilobatum fruits extract and its antibacterial, cytotoxic activity against human breast cancer cell line MCF 7. Spectrochim. Acta – Part A Mol Biomol. Spectrosc. 140, 223–228. https://doi.org/10.1016/j.saa.2014.12.060.
Sankar, R., Rizwana, K., Shivashangari, K.S., Ravikumar, V., 2015. Ultra-rapid photocatalytic activity of Azadirachta indica engineered colloidal titanium dioxide nanoparticles. Appl. Nanosci. 5, 731–736. https://doi.org/10.1007/s13204-014-0369-3.
Siddiqui, M.A., Singh, G., Kashyap, M.P., Khanna, V.K., Yadav, S., Chandra, D., Pant, A. B., 2008. Influence of cytotoxic doses of 4-hydroxynonenal on selected neurotransmitter receptors in PC-12 cells. Toxicol. Vitr. 22, 1681–1688. https://doi.org/10.1016/j.tiv.2008.07.001.
Sundrarajan, M., Gowri, S., 2011. Green synthesis of titanium dioxide nanoparticles by nyctanthes arbor-tristis leaves extract. Chalcogenide Lett. 8, 447–451.
Usman, M., Zaki, M., Khan, R.A., Alsalme, A., Ahmad, M., Tabassum, S., 2017. Coumarin centered copper(II) complex with appended-imidazole as cancer chemotherapeutic agents against lung cancer: molecular insight: Via DFT-based vibrational analysis. RSC Adv. 7, 36056–36071. https://doi.org/10.1039/c7ra05874h.
Zaman, M., Ahmad, E., Qadeer, A., Rabbani, G., Khan, R.H., 2014. Nanoparticles in relation to peptide and protein aggregation. Int. J. Nanomed. 9, 899–912. https://doi.org/10.2147/IJN.S54171.
Zaman, M., Ehtram, A., Chaturvedi, S.K., Nusrat, S., Khan, R.H., 2016. Amyloidogenic behavior of different intermediate state of stem bromelain: a biophysical insight. Int. J. Biol. Macromol. 91, 477–485. https://doi.org/10.1016/j.ijbiomac.2016.05.107.
Zhang, H., Wang, G., Chen, D., Lv, X., Li, J., 2008. Tuning photoelectrochemical performances of Ag–TiO_2 nanocomposites via reduction-oxidation of Ag. Chem. Mater., 6543–6549